ISSN: 2414-1895 DOI: 10.6919/ICJE.202511_11(11).0001

Synthesis and Corrosion Inhibition Performance Evaluation of 4-Pyridinecarboxaldehyde-1,4-phenylenediamine Mono-Schiff Base

Yuanfang Deng[1], Junlan Li[2], Yue Li[2], Yutong Wei[2], Li Li[2], Yu Zhang[2], Jiawang Shen[2], Jing Zhou[2], Chuan Lai[2], Ting Long[2,*]

[1] Dazhou Market Supervision and Administration Bureau, Dazhou 635000, China

[2] Dazhou Key Laboratory of Advanced Technology for Fiber Materials, Basalt Fiber and Composite Materials Key Laboratory of Sichuan Province, Special Polymer Materials for Automobile Key Laboratory of Sichuan Province, Sichuan Institute of Arts and Science, Dazhou 635000, China

*Corresponding authors E-mail addresses: 610304548@qq.com (Ting Long)

Abstract

A planar rigid mono-Schiff base corrosion inhibitor, 4-pyridinecarboxaldehyde-1,4-phenylenediamine (PAM-4), was synthesized in this work. Nuclear magnetic resonance (NMR) spectroscopy confirmed the structure of the compound. The inhibitory effect of PAM-4 on mild steel in 1 mol/L HCl at 25°C, 35°C, and 45°C was assessed through weight loss measurements and electrochemical techniques. Scanning electron microscopy (SEM) was used to examine the surface morphology of mild steel before and after corrosion, demonstrating that PAM-4 provides effective protection. The results reveal that inhibitor concentration and temperature are key factors influencing performance. Inhibition efficiency improved with increasing PAM-4 concentration, achieving a maximum of 91.51% at 1600 mg/L. Conversely, elevated temperatures reduced the inhibition effect.

Keywords

Corrosion; Corrosion Inhibitor; Mono-Schiff Base; Mild Steel; Corrosion Inhibition Performance.

1. Introduction

Mild steel is widely utilized due to its excellent ductility, plasticity, and electrical conductivity. However, its susceptibility to corrosion limits its service life and performance. Metal corrosion causes significant economic losses; according to statistics, the global direct economic loss due to metal corrosion is approximately 700-1000 billion US dollars annually. Corrosion damage to metal materials, equipment, or structures can lead to factory shutdowns, leaks from corroded pipelines and equipment polluting the environment and endangering human health, and accidents involving the transport of flammable and explosive materials through pipelines due to corrosion can cause casualties. [1-10]

Currently, methods for preventing metal corrosion can be broadly classified into electrochemical protection, metal surface treatment, alloying, and adding corrosion inhibitors. Among these, adding corrosion inhibitors is one of the more common methods. Corrosion inhibitors, adhering to the metal surface at appropriate concentrations and forms, provide protection by preventing or slowing down the corrosion rate of metal materials. Their advantages include low dosage, significant effect, stable

ISSN: 2414-1895 DOI: 10.6919/ICJE.202511_11(11).0001

performance, simple operation, high efficiency, and high inhibition rate. However, current inhibitors face challenges such as P and S pollution, unpleasant odors, complex use, and difficult preparation. Therefore, the development of new green, efficient, and non-toxic corrosion inhibitors has become an important topic in metal corrosion inhibition. [11-17]

Schiff base structures contain N heteroatoms and readily form conjugated structures with aromatic rings and O atoms, making them important candidates for metal corrosion inhibitors. Currently, Schiff base compounds and their metal complexes are widely used in fields such as corrosion protection, catalysis, analysis, and medicine. Although some studies have applied Schiff bases to metal corrosion inhibition, most focus on corrosion inhibition for metals like Cu and Mg. There are few existing reports on the use of Schiff bases for corrosion inhibition of mild steel, particularly during the pickling process. [18-19]

This study used 4-pyridinecarboxaldehyde and p-phenylenediamine as raw materials to prepare a novel organic corrosion inhibitor, 4-pyridinecarboxaldehyde-1,4-phenylenediamine mono-Schiff base. The corrosion inhibition performance of the synthesized mono-Schiff base for mild steel in acidic solution (1 mol/L HCl) was evaluated using electrochemical methods [16] and the weight loss method.

2. Experimental

2.1 Reagents and Materials

All chemicals were analytical grade from Chengdu Kelong Chemical Co., Ltd. and used as received. A 1 mol/L HCl solution was prepared from 37% HCl. The mild steel samples contained: C 0.24%, Si 0.38%, Mn 0.17%, P and S < 0.01%, with the balance being Fe. Specimens sized 2.5 cm × 0.5 cm × 5.0 cm were used for weight loss tests.

2.2 Synthesis of 4-Pyridinecarboxaldehyde-1,4-phenylenediamine

According to the reaction in Figure 1, p-phenylenediamine (2.7 g) was dissolved in anhydrous ethanol in a three-necked flask. Then, pyridine-4-carboxaldehyde (2.35 ml) was added dropwise to the dissolved p-phenylenediamine, and the reaction proceeded at room temperature for four hours. After the reaction, the product was washed and suction filtered. After drying, 2.6 g of a yellow powdery product was obtained.

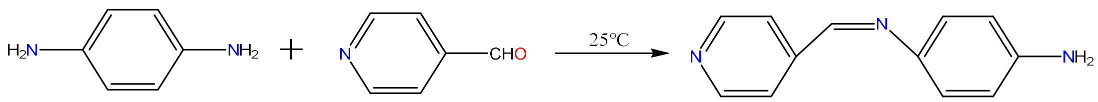

Figure 1. Reaction equation for the synthesis of 4-pyridinecarboxaldehyde-1,4-phenylenediamine mono-Schiff base.

2.3 Corrosion Inhibition Performance Testing

2.3.1 Weight Loss Method

The weight loss method was used to study the inhibition efficiency of PAM-4 for mild steel specimens in 1 mol/L HCl solution at different temperatures. For each temperature, six different concentration gradients of the inhibitor solution were set (0 mg/L, 100 mg/L, 400 mg/L, 800 mg/L, 1200 mg/L, 1600 mg/L). The immersion time for weight loss was 5 hours. After immersion, the mild steel coupons were rinsed with distilled water, degreased with acetone, and reweighed. The weight loss was calculated as the difference in weight before and after immersion.

2.3.2 Electrochemical Method

A CHI760E electrochemical workstation with a three-electrode system was employed. The setup included a mild steel working electrode, a saturated calomel reference electrode, and a platinum counter electrode. Tests involved open circuit potential (OCP) measurement for 1200 s,

ISSN: 2414-1895 DOI: 10.6919/ICJE.202511_11(11).0001

electrochemical impedance spectroscopy (EIS) from 10^{-2} to 10^5 Hz at 10 mV amplitude, and Tafel polarization scanning from −0.25 V to +0.25 V vs. OCP at 0.5 mV/s.

2.3.3 Surface Morphology Analysis

Morphology analysis was performed using scanning electron microscopy (SEM). Sample treatment followed the weight loss experiment procedure. The surface morphology of mild steel samples without and with the added inhibitor at different temperatures was observed and analyzed using SEM to visually assess the corrosion inhibition performance of PAM-4 on mild steel.

3. Results and Discussion

3.1 NMR Structural Characterization

Figure 2 shows the NMR results for PAM-4. ^{1}H NMR (600 MHz, DMSO-d_6): δ 8.71-8.68 (m, 2H), 8.66 (s, 1H), 7.79-7.75 (m, 2H), 7.28-7.21 (m, 2H), 6.68-6.60 (m, 2H), 5.47 (s, 2H). Among these, the multiplet at δ 8.71-8.68 corresponds to the two H atoms on the carbon atoms adjacent to the N atom in the pyridine ring, the singlet at δ 8.66 corresponds to the H atom on the C=N double bond, the multiplet at δ 7.79-7.75 corresponds to the two H atoms on the pyridine ring, the multiplet at δ 7.28-7.21 corresponds to the two H atoms on the benzene ring, the multiplet at δ 6.68-6.60 corresponds to the two H atoms on the benzene ring, and the singlet at δ 5.47 corresponds to the two H atoms on the H_2N- group. Based on the ^{1}H NMR spectrum, the successful synthesis of the target molecule was confirmed.

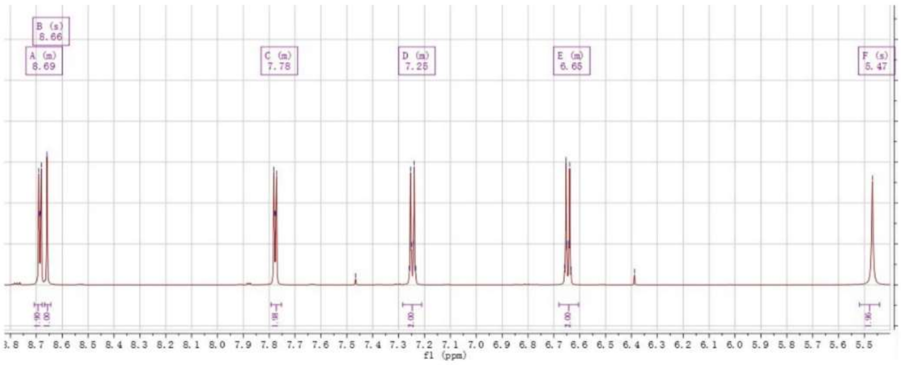

Figure 2. ^{1}H NMR spectrum of 4-pyridinecarboxaldehyde-1,4-phenylenediamine.

3.2 Electrochemical Data Analysis

3.2.1 Electrochemical Impedance Spectroscopy

Electrochemical impedance spectroscopy (EIS) is a non-destructive and reliable technique for exploring corrosion inhibition, surface passivation, and charge transfer mechanisms at the metal/solution interface. Figure 3 (a-f) shows the Nyquist and Bode plots obtained from EIS at different inhibitor concentrations and temperatures of 25°C, 35°C, and 45°C. As shown in Figure 3 (a): The curves are semicircular, and as the inhibitor concentration increases, the diameter of the semicircular arc also increases. Compared to the blank impedance complex plane, after adding the inhibitor, the radius of the capacitive loop in the high-frequency region increases, indicating an increase in the charge transfer resistance (Rct) and a decrease in the interfacial capacitance. This is mainly because the inhibitor particles replace water molecules on the surface of the carbon steel electrode, changing the interface layer between the carbon steel electrode and the solution from a water molecule layer to an inhibitor particle layer, thereby hindering the reaction between H^+ in the HCl system and Fe atoms on the mild steel surface, thus inhibiting the metal corrosion process and providing a protective effect [17]. As the temperature increases, the diameters of the semicircular arcs in Figure 3 (b) and (c) decrease. The inhibition efficiency also decreases with increasing temperature, primarily because the increase in temperature enhances the activity of acid protons, accelerating the diffusion process of H^+ and the electrode reaction rate, consequently increasing the corrosion rate.

ISSN: 2414-1895
DOI: 10.6919/ICJE.202511_11(11).0001

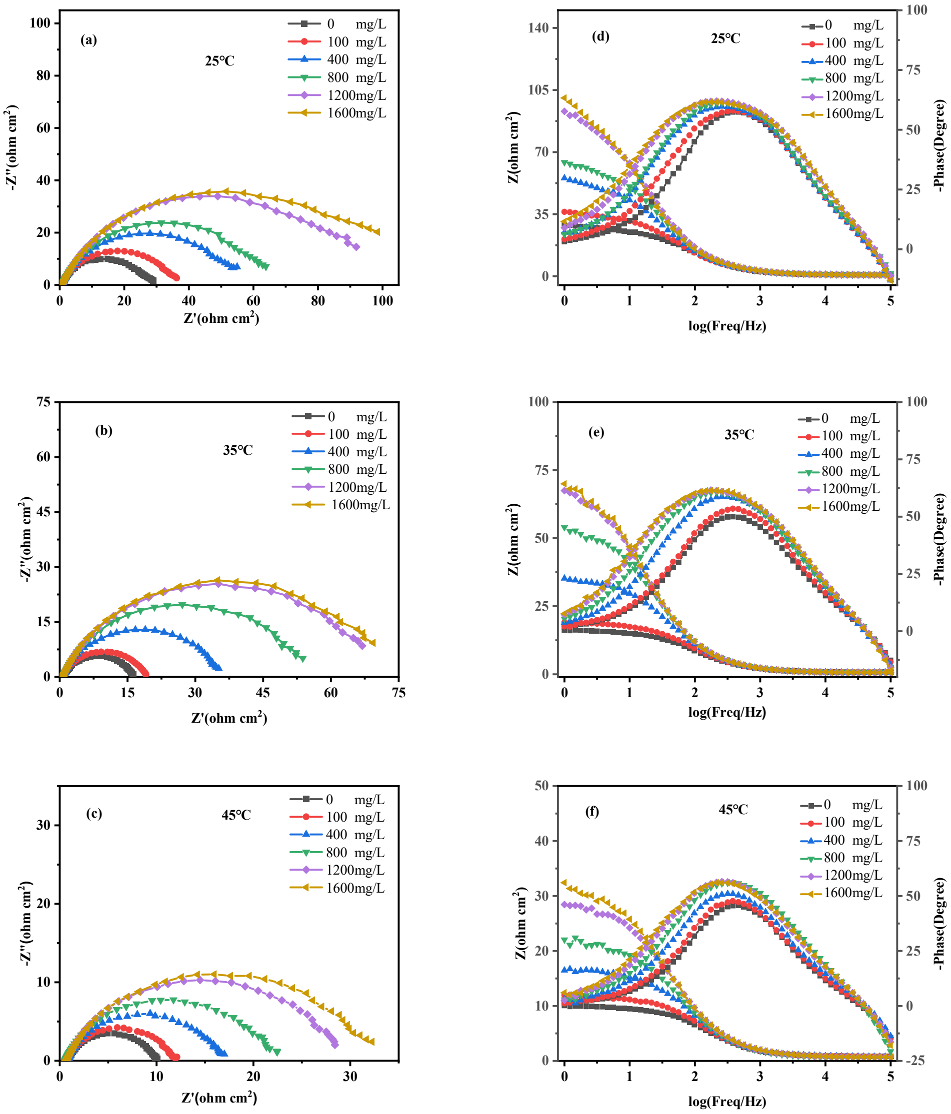

Figure 3. Nyquist and Bode plots with different inhibitor concentrations at different temperatures. (a), (b), (c) represent Nyquist plots at 25°C, 35°C, and 45°C, respectively. (d), (e), (f) represent Bode plots at 25°C, 35°C, and 45°C, respectively.

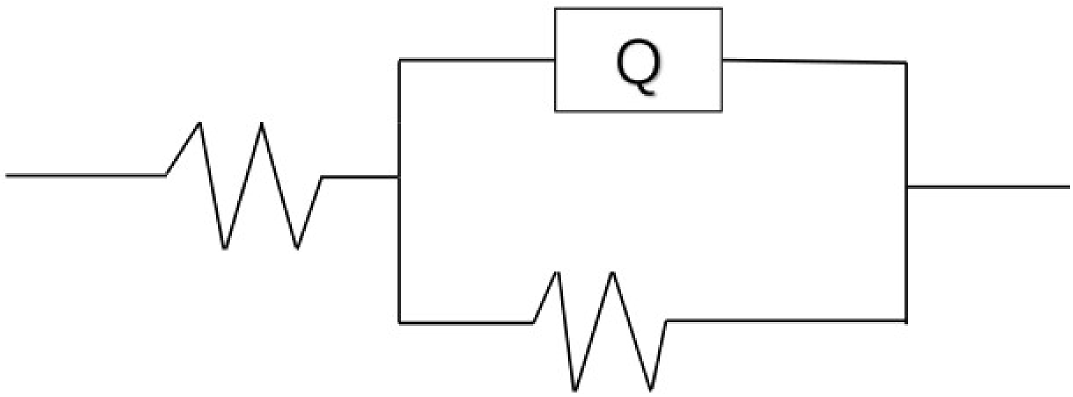

Figure 4. Equivalent circuit used for fitting.

Table 1. Impedance fitting parameters for mild steel in 1 mol/L HCl solution.

T(℃)	mg/L	$R_S(\Omega\ cm^2)$	n	$Y_0(\mu\Omega^{-1}S^n\ cm^{-2})$	$R_{ct}(\Omega\ cm^2)$	χ^2	η_w (%)
25℃	0	0.7733	0.8386	2.776	19.96	0.004206	-
	100	0.7651	0.8190	3.321	34.92	0.004220	42.79
	400	0.7762	0.8133	3.438	53.53	0.004368	62.71
	800	0.7989	0.8207	3.001	63.26	0.002962	68.44
	1200	0.7165	0.8030	3.238	93.52	0.004069	78.66
	1600	0.6932	0.7898	3.761	136.5	0.005634	85.38
35℃	0	0.8003	0.8187	4.620	11.34	0.003811	-
	100	0.7617	0.8293	4.008	18.91	0.004016	40.03
	400	0.6929	0.8272	3.954	27.37	0.005981	58.56
	800	0.7279	0.8148	4.113	34.12	0.005566	66.76
	1200	0.6649	0.7866	4.470	45.69	0.006351	75.18
	1600	0.6630	0.8066	4.487	59.1	0.007110	80.81
45℃	0	0.8571	0.8468	4.516	6.61	0.004150	-
	100	0.8454	0.8412	4.569	10.88	0.004370	39.25
	400	0.8064	0.8215	5.548	13.83	0.004113	52.21
	800	0.5809	0.8252	4.819	18.98	0.009164	65.17
	1200	0.7053	0.8139	4.967	24.92	0.005598	73.48
	1600	0.6940	0.7991	5.548	28.92	0.006818	77.14

The fitting parameters obtained using the R(QR) equivalent circuit shown in Figure 4 are listed in Table 1. These include: R_s (Ω cm²) solution resistance; n phase shift; χ^2 goodness of fit; Rct (Ω cm²) charge transfer resistance; Y_0 ($\mu\Omega^{-1}$ S^n cm^{-2}) constant phase element constant; η (%) inhibition efficiency. The inhibition efficiency η (%) was calculated according to the formula:

$$\eta(\%) = \frac{R - R_0}{R} \times 100\% \tag{1}$$

From the data in Table 1, it can be seen that the inhibitor concentration gradient has a significant impact on the inhibition effect. However, when the inhibitor reaches a certain concentration, the inhibition effect deteriorates, which is due to saturation of the inhibitor. Furthermore, at 25°C, the optimal inhibition efficiency of the inhibitor is 85.83%; at 35°C, it is 80.81%; and at 45°C, it is 77.14%. Therefore, the corrosion inhibition effect of 4-pyridinecarboxaldehyde-1,4-phenylenediamine mono-Schiff base on mild steel in 1 mol/L hydrochloric acid solution is negatively correlated with temperature.

3.2.2 Polarization Curves

Figure 5 (a), (b), (c) show the polarization curves of mild steel in 1 mol/L HCl solution with different concentrations of PAM-4, respectively. As the inhibitor concentration increases, both the cathodic and anodic polarization curves shift negatively, indicating that this inhibitor is a mixed-type inhibitor (affecting both cathodic and anodic reactions) [18].

ISSN: 2414-1895
DOI: 10.6919/ICJE.202511_11(11).0001

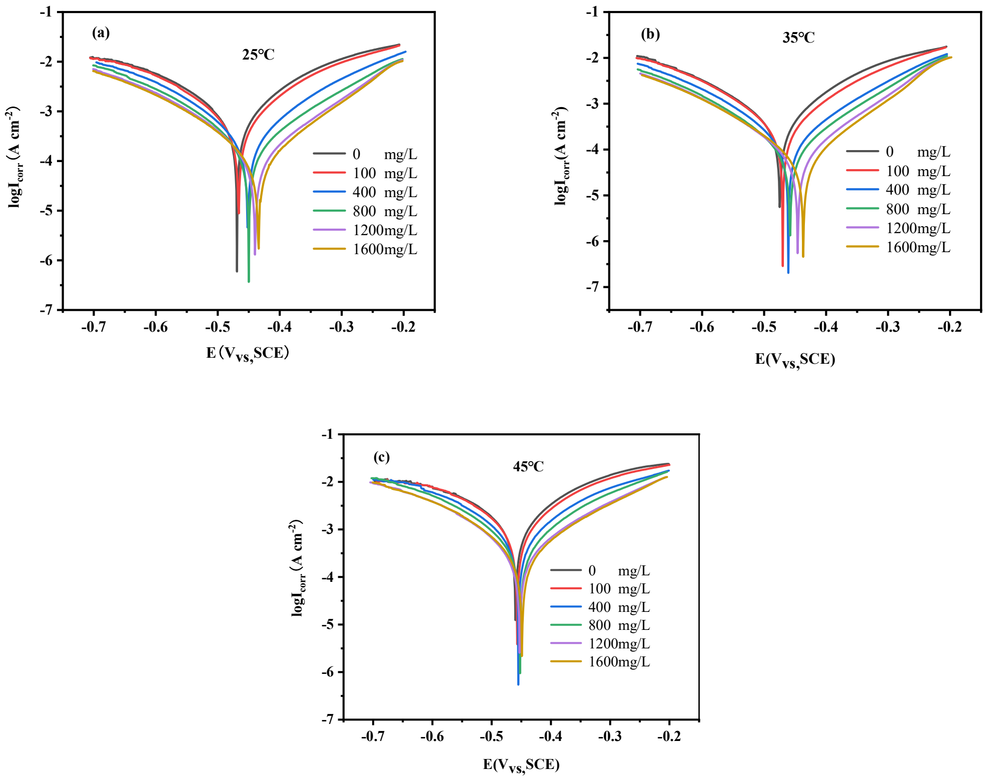

Figure 5. Polarization curves with different inhibitor concentrations at different temperatures.

Table 2. Polarization curve fitting parameters for mild steel in 1 mol/L HCl solution at different temperatures and inhibitor concentrations.

T(℃)	mg/L	I_{corr}(μA cm^{-2})	-β_c(mv dec)	β_a(mv dec)	E_{corr}(v)	η_w (%)
25℃	0	383.5	-3.453	3.407	-0.475	-
	100	215.16	-3.547	3.533	-0.470	43.90
	400	149.6	-3.879	3.826	-0.461	60.99
	800	90.25	-4.044	4.012	-0.458	76.46
	1200	68.58	-4.173	4.167	-0.446	82.82
	1600	53.22	-4.245	4.230	-0.437	86.12
35℃	0	739.4	-3.147	3.125	-0.469	-
	100	439.2	-3.277	3.226	-0.466	40.60
	400	300.2	-3.427	3.395	-0.458	59.40
	800	193.2	-3.795	3.706	-0.450	73.87
	1200	129.8	-3.970	3.874	-0.440	82.45
	1600	112.5	-4.330	3.958	-0.434	84.78
45℃	0	1506	-2.883	2.847	-0.460	-
	100	926.8	-2.972	2.964	-0.457	38.50
	400	693.4	-3.207	3.187	-0.455	53.96
	800	741.0	-3.373	3.332	-0.452	68.73
	1200	329.8	-3.488	3.488	-0.453	78.10
	1600	307.4	-3.522	3.522	-0.449	79.59

ISSN: 2414-1895
DOI: 10.6919/ICJE.202511_11(11).0001

Table 2 (continued) Polarization curve fitting parameters for mild steel in 1 mol/L HCl solution at different temperatures and inhibitor concentrations.

Specific polarization parameters are listed in Table 2. These include corrosion potential (E_{corr}), anodic Tafel slope (β_a), cathodic Tafel slope (β_c), corrosion current density (I_{corr}), and inhibition efficiency (η). The inhibition efficiency calculated from polarization curves [19] uses the formula:

$$\eta = [(I_0 - I)/I_0] \times 100\% \quad (2)$$

Where: I_0 is the corrosion current density without inhibitor; I_{corr} is the corrosion current density with inhibitor.

As the inhibitor concentration increases, the inhibition efficiency gradually increases. When the inhibitor concentration reaches 1600 mg/L, the optimal inhibition efficiency at 25°C is 86.12%; at 35°C it is 84.78%, and at 45°C it is 79.59%. These results are consistent with the electrochemical impedance results. This proves that the addition of PAM-4 effectively inhibits the corrosion of mild steel in 1 mol/L HCl solution. Furthermore, the changes in the anodic and cathodic Tafel slopes for mild steel in 1 mol/L HCl solution with PAM-4 are almost identical, and the corresponding corrosion potential changes are small. Thus, it can be concluded that PAM-4 acts as a mixed-type inhibitor under these conditions.

3.3 Weight Loss Method

To further verify the accuracy of the electrochemical experiments, weight loss experiments were conducted. As shown in Figure 6, as the concentration of the Schiff base inhibitor solution increases, the inhibition efficiency also increases. However, when the concentration reaches a certain level, the inhibition efficiency levels off, primarily because the inhibitor solution reaches saturation and the effect stabilizes. When the inhibitor concentration gradient is fixed, increasing the temperature also increases the corrosion rate, indicating that temperature also has a significant influence on the inhibition efficiency.

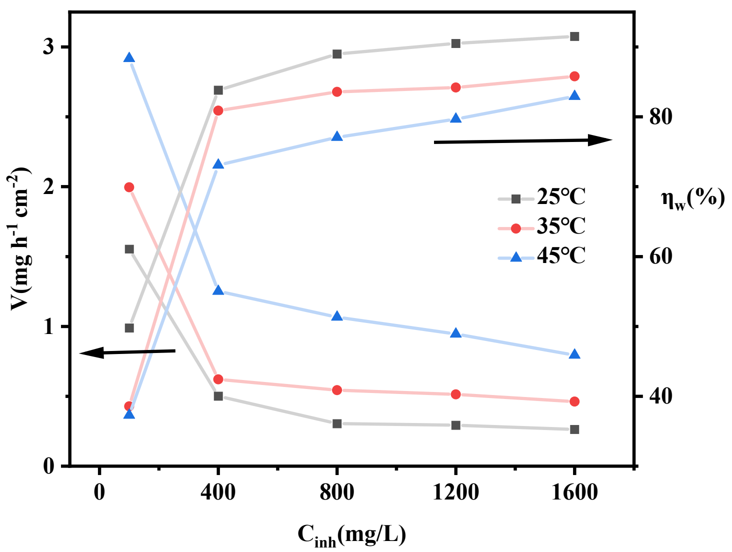

Figure 6. Inhibition efficiency of 4-pyridinecarboxaldehyde-1,4-phenylenediamine at different concentrations and different temperatures.

ISSN: 2414-1895 DOI: 10.6919/ICJE.202511_11(11).0001

Table 3. Weight loss data for mild steel in 1 mol/L HCl solution at different inhibitor concentrations and temperatures.

T(℃)	mg/L	V_{ihn}(mg h^{-1} cm^{-2})	η_w(%)	θ
25℃	0	3.093	0	0
	100	1.5534	49.78	0.4978
	400	0.501	83.80	0.8380
	800	0.3048	88.99	0.8899
	1200	0.2932	90.52	0.9052
	1600	0.2626	91.51	0.9151
35℃	0	3.249	0	0
	100	1.996	38.57	0.3857
	400	0.6208	80.98	0.8098
	800	0.5444	83.57	0.8357
	1200	0.5138	84.19	0.8419
	1600	0.4618	85.79	0.8579
45℃	0	4.652	0	0
	100	2.917	37.30	0.3730
	400	1.2512	73.10	0.7310
	800	1.0666	77.07	0.7707
	1200	0.9454	79.68	0.7968
	1600	0.7961	82.92	0.8292

Table 3 presents the corrosion inhibition performance data for mild steel at different temperatures and inhibitor concentrations, including the corrosion rate (V_{inh} (mg h^{-1} cm^{-2})) and inhibition efficiency (η_w %). The corresponding calculations use the following formulas:

$$V = [(m_0 - m)]/st \quad (3)$$

$$\eta_W(\%) = [(v_0 - v)/v_0] \times 100\% \quad (4)$$

Where: m_0 and m are the masses of the specimen before and after corrosion, respectively, in g; S is the exposed surface area, in cm^2; t is the immersion time, in h; V_0 and V_{inh} are the corrosion rates of the mild steel specimen in HCl solution without inhibitor and with different concentrations of inhibitor at the test time, respectively.

As shown in Table 3, which displays the weight loss test results for mild steel in 1 mol/L HCl solution, as the concentration of added PAM-4 increases, the weight loss of mild steel decreases, the corrosion rate decreases, the inhibition efficiency increases, and the inhibition effect improves. From the table,

ISSN: 2414-1895 DOI: 10.6919/ICJE.202511_11(11).0001

it can be seen that at 25°C, when the inhibitor concentration reaches 1600 mg/L, the inhibition efficiency for mild steel reaches 91.51%; at 35°C, with 1600 mg/L inhibitor, the inhibition efficiency is 85.79%; and at 45°C, with 1600 mg/L inhibitor, the inhibition efficiency still reaches 82.92%. This analysis shows that as the temperature increases, even at the same concentration, the inhibition effect worsens. Therefore, temperature also determines the corrosion inhibition effect of PAM-4. This is mainly because as the temperature rises, the activity of acid protons increases, intensifying the corrosion degree of mild steel. These results are consistent with those obtained electrochemically, verifying the accuracy of the electrochemical results.

3.4 Surface Morphology Analysis

Figure 7 shows the SEM results for samples with and without the added inhibitor at various temperatures. As seen in Figure 7 (b), (d), (f), when no inhibitor is added to the 1 mol/L HCl solution, the surface of the mild steel is extensively oxidized and damaged by the acidic medium. In contrast, in Figure 7 (c), (e), (g) with the added inhibitor, the mild steel surface appears relatively smooth, because the inhibitor forms a protective film on the mild steel surface. This protective film acts as a barrier, isolating the corrosion-prone mild steel surface from the corrosive environment, thereby reducing the corrosion rate of the mild steel. However, from the figures, it can be observed that as the temperature increases, the surface quality of the carbon steel deteriorates, regardless of whether the inhibitor is added or not. Thus, temperature directly affects the corrosion rate. This is consistent with the conclusions drawn from the weight loss and electrochemical methods.

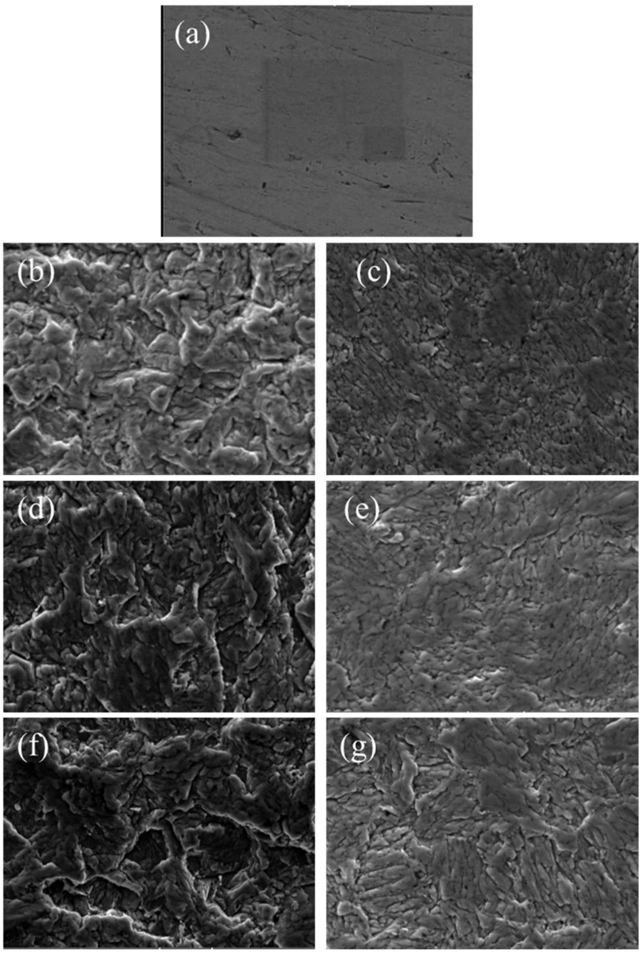

Figure 7. Mild steel samples with and without inhibitor at different temperatures. (a) Blank control group. (b), (d), (f) represent mild steel samples without inhibitor at 25°C, 35°C, and 45°C, respectively. (c), (e), (g) represent carbon steel samples with inhibitor at 25°C, 35°C, and 45°C, respectively.

ISSN: 2414-1895 DOI: 10.6919/ICJE.202511_11(11).0001

4. Conclusion

This study synthesized a planar rigid mono-Schiff base corrosion inhibitor, 4-pyridinecarboxaldehyde-1,4-phenylenediamine (PAM-4). The structure of the synthesized mono-Schiff base was characterized by NMR spectroscopy. Its corrosion inhibition effect on mild steel in 1 mol/L HCl at 25°C, 35°C, and 45°C was evaluated using weight loss and electrochemical methods. The results show that the corrosion inhibition performance of PAM-4 for mild steel in 1 M HCl is negatively correlated with temperature and positively correlated with its concentration. Polarization curve results indicate that PAM-4 is a mixed-type inhibitor, capable of inhibiting both the cathodic hydrogen evolution reaction and the anodic dissolution of mild steel in 1 M HCl. The weight loss results show that the optimal inhibition efficiency of PAM-4 is 91.51% (at 1600 mg/L). Surface morphology analysis of the mild steel before and after corrosion by SEM confirmed that the prepared inhibitor has good corrosion inhibition performance for mild steel. These findings can be well applied to the metal pickling process and provide data and theoretical support for the development and research of pickling corrosion inhibitors.

Date Availability

The data that support the findings of this study are available. All data generated or analyzed during this study are included in this published article.

Credit Authorship Contribution Statement

Yuanfan Deng, Ting Long, Junlan Li and Li Li performed the experiments and analyzed the data with the help from Yu Zhang. Jiawang Shen and Yue Li: Investigation, Conceptualization. Yutong Wei and Jin Zhou: Investigation.

Acknowledgments

Declaration of Funding: Authors would like to appreciate the financial support from Market Supervision Administration of Sichuan Province (SCSJZ2025014), Natural Science Foundation of Sichuan (General Program; 2024NSFSC2031), Bureau of Science and Technology of Dazhou (24YYJC0003, 2024SSZXDWHZ01), National Natural Gas Product Quality Supervision and Inspection Center (Sichuan; GJKFJJ001).

Competing Interests

All the authors declare that they have no conflict of interest.

References

[1] El Azzouzi, M., Azzaoui, K., Warad, I., Hammouti, B., Shityakov, S., Sabbahi, R., ... & Zarrouk, A. (2022). Moroccan, Mauritania, and senegalese gum Arabic variants as green corrosion inhibitors for mild steel in HCl: Weight loss, electrochemical, AFM and XPS studies. Journal of Molecular liquids, 347, 118354.

[2] Kumar, H., & Dhanda, T. (2021). Cyclohexylamine an effective corrosion inhibitor for mild steel in 0.1 N H2SO4: experimental and theoretical (molecular dynamics simulation and FMO) study. Journal of Molecular Liquids, 327, 114847.

[3] Hegazy, M. A., El-Tabei, A. S., Bedair, A. H., & Sadeq, M. A. (2015). Synthesis and inhibitive performance of novel cationic and gemini surfactants on carbon steel corrosion in 0.5 M H_2SO_4 solution.

[4] Jeeva, M., Prabhu, G. V., Boobalan, M. S., & Rajesh, C. M. (2015). Interactions and inhibition effect of urea-derived Mannich bases on a mild steel surface in HCl. The Journal of Physical Chemistry C, 119(38), 22025-22043.

[5] Murthy, R., Gupta, P., & Sundaresan, C. N. (2020). Theoretical and electrochemical evaluation of 2-thioureidobenzheteroazoles as potent corrosion inhibitors for mild steel in 2 M HCl solution. Journal of Molecular Liquids, 319, 114081.

[6] Golchinvafa, A., Anijdan, S. M., Sabzi, M., & Sadeghi, M. (2020). The effect of natural inhibitor concentration of Fumaria officinalis and temperature on corrosion protection mechanism in API X80 pipeline steel in 1 M H2SO4 solution. International Journal of Pressure Vessels and Piping, 188, 104241.

[7] Bedair, M. A., El-Sabbah, M. M. B., Fouda, A. S., & Elaryian, H. M. (2017). Synthesis, electrochemical and quantum chemical studies of some prepared surfactants based on azodye and Schiff base as corrosion inhibitors for steel in acid medium. Corrosion science, 128, 54-72.

[8] Kalaiselvi, P., Chellammal, S., Palanichamy, S., & Subramanian, G. (2010). Artemisia pallens as corrosion inhibitor for mild steel in HCl medium. Materials Chemistry and Physics, 120(2-3), 643-648.

[9] Fakhry, H., El Faydy, M., Benhiba, F., Laabaissi, T., Bouassiria, M., Allali, M., ... & Zarrouk, A. (2021). A newly synthesized quinoline derivative as corrosion inhibitor for mild steel in molar acid medium: Characterization (SEM/EDS), experimental and theoretical approach. Colloids and Surfaces A: Physicochemical and Engineering Aspects, 610, 125746.

[10] Ehsani, A., Mahjani, M. G., Moshrefi, R., Mostaanzadeh, H., & Shayeh, J. S. (2014). Electrochemical and DFT study on the inhibition of 316L stainless steel corrosion in acidic medium by 1-(4-nitrophenyl)-5-amino-1 H-tetrazole. RSC Advances, 4(38), 20031-20037.

[11] Fernandes, C. M., Alvarez, L. X., dos Santos, N. E., Barrios, A. C. M., & Ponzio, E. A. (2019). Green synthesis of 1-benzyl-4-phenyl-1H-1, 2, 3-triazole, its application as corrosion inhibitor for mild steel in acidic medium and new approach of classical electrochemical analyses. Corrosion Science, 149, 185-194.

[12] Lgaz, H., Salghi, R., & Ali, I. H. (2018). Corrosion inhibition behavior of 9-hydroxyrisperidone as a green corrosion inhibitor for mild steel in hydrochloric acid: electrochemical, DFT and MD simulations studies. International Journal of Electrochemical Science, 13(1), 250-264.

[13] Pandey, A., Singh, B., Verma, C., & Ebenso, E. E. (2017). Synthesis, characterization and corrosion inhibition potential of two novel Schiff bases on mild steel in acidic medium. RSC advances, 7(74), 47148-47163.

[14] Gupta, R. K., Malviya, M., Verma, C., & Quraishi, M. A. (2017). Aminoazobenzene and diaminoazobenzene functionalized graphene oxides as novel class of corrosion inhibitors for mild steel: experimental and DFT studies. Materials Chemistry and Physics, 198, 360-373.

[15] Murmu, M., Saha, S. K., Murmu, N. C., & Banerjee, P. (2019). Effect of stereochemical conformation into the corrosion inhibitive behaviour of double azomethine based Schiff bases on mild steel surface in 1 mol L− 1 HCl medium: An experimental, density functional theory and molecular dynamics simulation study. Corrosion Science, 146, 134-151.

[16] Erami, R. S., Amirnasr, M., Meghdadi, S., Talebian, M., Farrokhpour, H., & Raeissi, K. (2019). Carboxamide derivatives as new corrosion inhibitors for mild steel protection in hydrochloric acid solution. Corrosion Science, 151, 190-197.

[17] Heydari, H., Talebian, M., Salarvand, Z., Raeissi, K., Bagheri, M., & Golozar, M. A. (2018). Comparison of two Schiff bases containing O-methyl and nitro substitutes for corrosion inhibiting of mild steel in 1 M HCl solution. Journal of Molecular liquids, 254, 177-187.

[18] Talebian, M., Raeissi, K., Atapour, M., Fernández-Pérez, B. M., Salarvand, Z., Meghdadi, S., ... & Souto, R. M. (2018). Inhibitive effect of sodium (E)-4-(4-nitrobenzylideneamino) benzoate on the corrosion of some metals in sodium chloride solution. Applied Surface Science, 447, 852-865.

[19] Dueke-Eze, C. U., Madueke, N. A., Iroha, N. B., Maduelosi, N. J., Nnanna, L. A., Anadebe, V. C., & Chokor, A. A. (2022). Adsorption and inhibition study of N-(5-methoxy-2-hydroxybenzylidene) isonicotinohydrazide Schiff base on copper corrosion in 3.5% NaCl. Egyptian Journal of Petroleum, 31(2), 31-37.